High-resolution, high-frequency wavelength shift detection of optical signals with low-cost, compact readouts

Schuh, A.; Hegyi, A.; Raghavan, A.; Lochbaum, A.; Schwartz, J.; Kiesel, P.

PARC, a Xerox Company, Palo Alto, CA 94304, USA

ABSTRACT

Fiber-optics (FO) have great potential for distributed sensing in various harsh environment applications. Their advantages include high resolution and multiplexing capabilities, inherent immunity to electromagnetic interference, and low weight/volume. However, their widespread adoption in commercial applications has been considerably limited by the high cost, size, weight, and lack of capabilities of the readout unit used to interpret the FO signals. PARC has developed a breakthrough wavelength shift detection (WSD) technology that is capable of reading out signals from wavelength-encoded FO and other optical sensors with high sensitivity using a compact, high-speed and low-cost unit. In this paper, its calibration and noise performance is demonstrated for high resolution (up to 1.45 fm/√Hz) acoustic emission (AE) detection of fast (up to 1 MHz) dynamic strain signals.

1. INTRODUCTION

Wavelength-encoded optical sensors have considerable potential for various laboratory characterization and fielded system-monitoring applications. However, their widespread adoption, particularly for field deployment, is still challenged by the cost, weight, size, and resolution of read-out units to interrogate them. To mitigate these issues, PARC has developed a low-cost, compact, and fast-response wavelength detector suitable for interrogating such wavelength-encoded optical sensors with unprecedented resolution. It is also useful to precisely determine the wavelength of light sources [1-4]. Applications include read-out of fiber sensors, photonic crystal sensors, laser cavity sensors and compact spectroscopy. The system combines a position-sensitive photo detector with an optical coating. The coating converts the wavelength information of the incident light into a spatial intensity distribution on the photo detector. Differential read-out of the photo detector allows the determination of the centroid of such distribution. In summary, PARC's readout converts wavelength shifts into a simple centroid detection scheme, which allows for much higher resolution and cut-off frequency for monitoring optical wavelengths than possible with conventional optical readouts.

Fiber Optic Sensors and Applications XII, edited by Gary Pickrell, Eric Udd, Henry H. Du, Proc. of SPIE Vol. 9480, 94800B · © 2015 SPIE
CCC code: 0277-786X/15/$18 · doi: 10.1117/12.2177478

Previous experimental high speed fiber optic detection approaches reported in the literature include tunable lasers [5], matched fiber Bragg grating (FBG) read-outs [6] and two-wave mixing interferometry [7] with noise levels of 40fm/√Hz, 15fm/√Hz and 71fm/√Hz, respectivly. With a tunable laser the wavelength is fixed such that it corresponds to the steepest slope of the grating reflection spectrum (at half maximum). A shift in the FBG spectrum will modulate the reflected light intensity and the reflected optical power is detected with a conventional photodiode. The matched FBG read-out works with broadband illumination, often using an amplified spontaneous emission source or a superluminescent LED. The principle employs a reference grating as demodulating element that translates the wavelength shift into an intensity signal. The two-wave mixing interferometer uses a coherent light source split into several sampling beams and a reference beam. In a single channel setup, the sampling beam is routed to the fiber sensor and both the reflected light and reference beam are pointed to a photorefractive crystal. The interference of both results in a grating formed in the crystal, at which the reference beam is diffracted. Careful alignment of both beams puts them in phase. After passing a phase retarding element and a polarizing beam splitter, the two polarization components are focused on a photodetector array and demodulated. Existing commercial detectors have relatively low speed (<5 kHz) and noise performance capabilities. Some of such instruments are MicronOptics sm130™ with 32fm/√Hz [8], National Instruments PXIe-4844™ with 317fm/√Hz [9] and BaySpec FBG Interrogation Analyzer™ with 28fm/√Hz [10].

An application of our fast read-out is the detection of acoustic emissions (AEs). AEs are dynamic strain signals, typically in the ultrasonic frequency regime. AE is defined in this context as the generation and propagation of transient ultrasonic elastic waves within a material due to the sudden release of localized energy within a solid [11]. High-resolution acoustic emission detection has several health monitoring applications. Examples include nondestructive and in-situ testing of battery cells [12] and aerospace structures [13]. Acoustic emissions can be detected in frequency ranges below 1 kHz and have been reported at frequencies up to 100 MHz. However, most of the released energy in damage monitoring is typically within the 1 kHz to 1 MHz range. Rapid stress-releasing events such as crack initiation and growth generate a spectrum of stress waves starting at 0 Hz, and are typically falling off at several MHz [11]. In this work, we demonstrate a novel detector for simulated acoustic emissions based on fiber optic sensing.

2. CONSTRUCTION AND CALIBRATION

The construction and calibration of the centroid detector is discussed in this section. The working principle is illustrated in Figure 1. The incoming light at wavelength λ_{in} is routed through a linear optical variable filter. Only wavelengths within a particular range are transmitted and collected by two photosensitive sensors I_1 and I_2. The difference of the signals of $I_1$and I_2 is normalized to the sum of the two (I_1+ I_2), which renders the signal strength independent of the light source. This makes it relatively robust to noise source fluctuations. As a result, the output voltage is proportional to the distribution of the light. The working principle of the centroid detector can be found in more detail in [14].

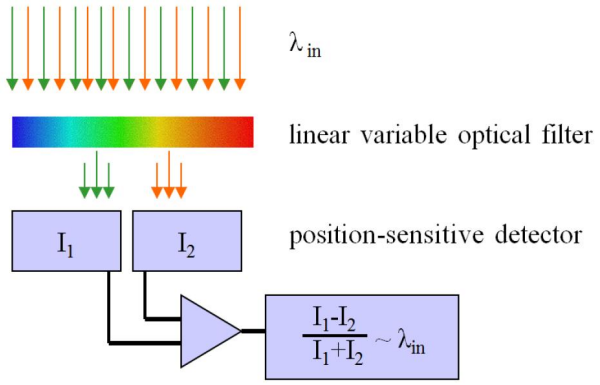

Figure 1: Working principle of detector based on differentiation and normalization.

The mechanical design of the wavelength centroid detector is briefly described in the following. While the optical signals are inherently immune to electromagnetic interference (EMI), the electronic detector circuit can be susceptible to it in the absence of appropriate shielding. To prevent EMI, the electronic detector circuit is placed inside an aluminum box. A photodiode is facing a hole in the cover to allow the incidence of light. A collimator holder serves for precise alignment of the light beam on the detector and linear optical filter. SMA connectors provide the "sum" and "difference" signals from the circuit. The detector's calibration is shown in Figure 2. In Figure 2(a), (I_1 - I_2) and (I_1 + I_2) are measured at different light source power settings. However, in Figure 2(b), all curves are similar after computing the normalized values (I_1 - I_2 / I_1 + I_2). This demonstrates the robustness of our approach to light source fluctuations.

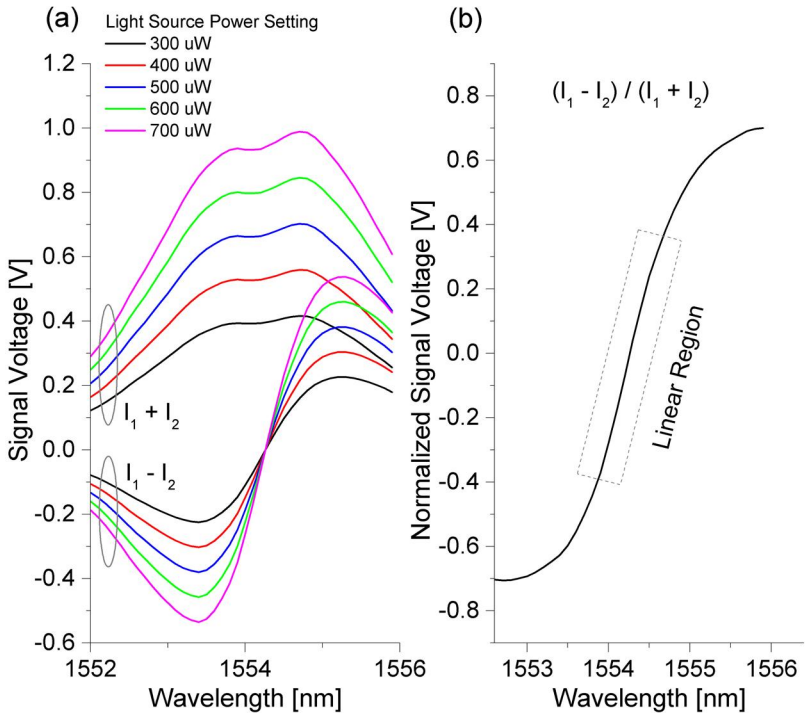

Figure 2: Calibration of centroid wavelength detector.

3. NOISE PERFORMANCE AT DIFFERENT READ-OUT SAMPLE RATES

The signals of the centroid detector are sampled with various different effective sample rates and compared to each other. In the calibrated setup a high power laser of 1 mW is used, tuned to 1559.111 nm. In all cases the sampling rates of the "sum" and "difference" signals are 2MS/s. They are then decimated to a desired sample rate by using an appropriate moving average filter and picking every x^{th} value based on the decimation factor x. Hence, the noise power is decreased with lower decimated effective sample rates. Figure 3 indicates the noise at an effective sample rate of 400 kHz with a noise Standard Deviation (SD) of 203.9 fm. The inset indicates the noise spectral density of the 400 kHz signal. Noise SDs experimentally obtained at other effective sample rates are: 29.9 fm (400 Hz), 31.5 fm (800 Hz), 38.8 fm (4 kHz), 44.7 fm (8 kHz), 69.6 fm (40 kHz), 89.7 fm (80 kHz) and 331.9 fm (1 MHz).

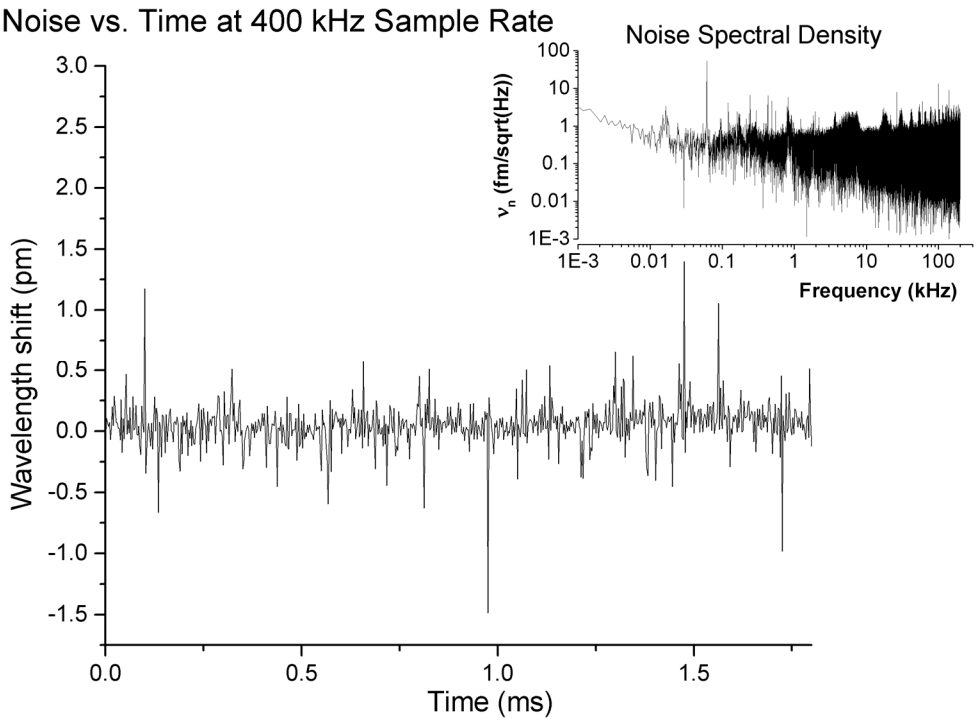

Figure 3: Noise performance at 400 kHz effective sample rate. The inset indicates the noise spectral density of the same signal.

4. CENTROID DETECTION WITH MODULATED LIGHT SIGNAL

A piezoelectric transducer excited at a center frequency of 8kHz is used to simulate mild acoustic emission events in an aluminum plate. The plate also has an FBG sensor at some distance from the piezoelectric transducer (Figure 4). Since the FBG itself is small in diameter (200 μm) relative to the host structure thickness (2 mm), its presence does not significantly affect the sensor signal. In

general, the acoustic emission spectrum and signal features depend on the host material and type of damage. Correspondingly, these features can be useful for damage characterization. However, since a source with known frequency characteristics is employed for the initial measurements reported here, a bandpass filter is used to reduce the measurement bandwidth to 4 kHz (from a frequency of 5 kHz to 9 kHz). The FBG source's laser power is 50 µW. Oversampling and subsequent decimation has been performed, resulting in a measured signal SD of 36.6 fm. This SD is lower than in Section 3 due to the lower measurement bandwidth, even by using a lower laser intensity. Overall, the measurement noise leads to a wavelength sensitivity better than 0.1 pm, as can be seen on the right scale of the plot in Figure 4. Further reduction in bandwidth by a factor of 100 towards 40 Hz can potentially lead to a wavelength resolution of 10 fm.

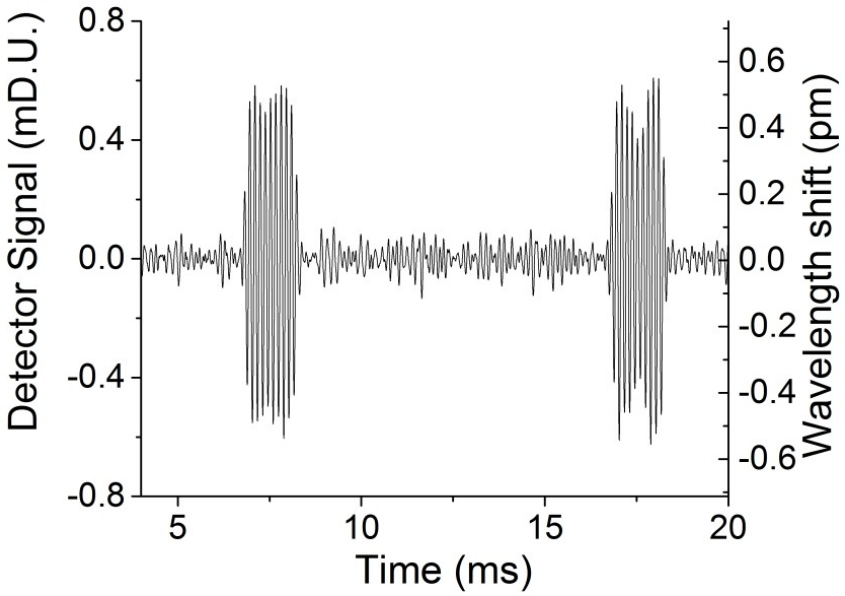

Figure 4 Wavelength centroid detector signal for an 8 kHz excitation signal (excitation amplitude 3 V), band pass filtered to a bandwidth of 4 kHz (from 5 to 9 kHz).

5. CONCLUSION

This study presents the extension, calibration, and operation of the PARC centroid wavelength shift detector for the detection of acoustic emissions. The sensitivity is a function of laser source power and decimation factor, amongst others. The measurement results reported here indicate that the wavelength centroid detector has a sensitivity <100 fm at low bandwidths. Further optimization can lead to signal bandwidths of > 1 MHz. Optical detection of simulated acoustic emission events excited by a piezoelectric transducer has been demonstrated. The measured wavelength sensitivity for the given detector setup (optical filter, photodiode, fiber Bragg grating, light source, etc.) is 1.45 fm / √Hz. The current prototype exceeds commercially available systems by at least one order of magnitude in terms of sensitivity. However, an improvement in sensitivity by a factor of 20 can potentially be achieved by optimized component characteristics and improved detector noise behavior. Future work will also address extension of this PARC technology for reading out

multiplexed optical signals with high resolution. Such multiplexing capabilities can facilitate damage source triangulation by enabling monitoring from multiple points, as well as easier scaling up to monitor the health of larger structures for civil and aerospace applications.

ACKNOWLEDGMENTS

The information, data, or work presented herein was funded in part by the Advanced Research Projects Agency - Energy (ARPA-E), U.S. Department of Energy, under Award Number DE-AR0000274.

REFERENCES

[1] P. Kiesel, O. Schmidt, and O. Wolst, “Using position-sensitive detectors for wavelength determination,” Dec. 18 2007, US Patent 7,310,153.

[2] O. Schmidt, P. Kiesel, S. Mohta, and N. M. Johnson, “Resolving pm wavelength shifts in optical sensing,” Applied Physics B, vol. 86, no. 4, pp. 593–600, 2007.

[3] P. Kiesel, O. Schmidt, N. Johnson et al., “Wavelength monitors for optical sensing applications optical sensors have many advantages, but before they can compete effectively in the $50 billion global sensor market, their prices have to drop.” Photonics Spectra, 2007.

[4] K. Bellmann, P. Kiesel, and N. Johnson, “Compact and fast read-out for wavelength-encoded biosensors,” in MOEMS-MEMS. International Society for Optics and Photonics, 2010, 7593: 759302.

[5] D. J.Webb, J. Surowiec, M. Sweeney, D. A. Jackson, L. Gavrilov, J. Hand, L. Zhang, and I. Bennion, "Miniature fiber optic ultrasonic probe," in SPIE's 1996 International Symposium on Optical Science, Engineering, and Instrumentation. International Society for Optics and Photonics, 1996, pp. 76-80.

[6] N. Takahashi, K. Yoshimura, and S. Takahashi, "Fiber bragg grating vibration sensor using incoherent light," Japanese Journal of Applied Physics, vol. 40, no. 5S, p. 3632, 2001.

[7] P. Fomitchov, T. W. Murray, and S. Krishnaswamy, "Intrinsic fiber-optic ultrasonic sensor array using multiplexed two-wave mixing interferometry."Applied optics, vol. 41, no. 7, pp. 1262-6, Mar. 2002.

[8] Micron Optics, "Datasheet sm130," May 2015. [Online]. Available: http://www.micronoptics.com/uploads/library/documents/datasheets/instruments/Micron Optics sm130.pdf

[9] National Instruments, "Datasheet NI PCIe-4844," May 2015. [Online]. Available: http://sine.ni.com/ds/app/doc/p/id/ds-338/lang/en

[10] BaySpec, "FBG Interrogation Analyzer," May 2015. [Online]. Available: http://www.bayspec.com/telecom-_ber-sensing/fbg-interrogation-analyzer/

[11] C. Scruby, "An introduction to acoustic emission," Journal of Physics E: Scientific Instruments, vol. 20, no. 8, p. 946, 1987.

[12] T. Ohzuku, H. Tomura, and K. Sawai, "Monitoring of particle fracture by acoustic emission during charge and discharge of Li/MnO2 cells," Journal of The Electrochemical Society, vol. 144, no. 10, pp. 3496-3500, 1997.

[13] R. D. Finlayson, M. Friesel, M. Carlos, P. Cole, and J. C. Lenain. “Health monitoring of aerospace structures with acoustic emission and acousto-ultrasonics,” *Insight-Wigston Then Northampton,* vol. 43, no. 3, pp. 155-158, 2001.

[14] T. Staudt, P. Kiesel, J. Martini, N. M. Johnson, C. Urbina, E. Burlbaw, “Compact wavelength monitor for remote sensing applications suitable to precisely measure the wavelength of individual laser pulses”, Proc. SPIE 8720, Photonic Applications for Aerospace, Commercial, and Harsh Environments IV, 87200P (May 31, 2013); doi:10.1117/12.2017959.